

AD-A078 923

STANFORD UNIV CALIF STANFORD ELECTRONICS LABS

F/8 4/1

ELF SPHERIC OCCURENCES IN THE ANTARCTIC DURING A SOLAR PROTON EV--FTC(U)

SEP 79 A C FRASER-SMITH , R A HELLIWELL

DNA001-78-C-0017

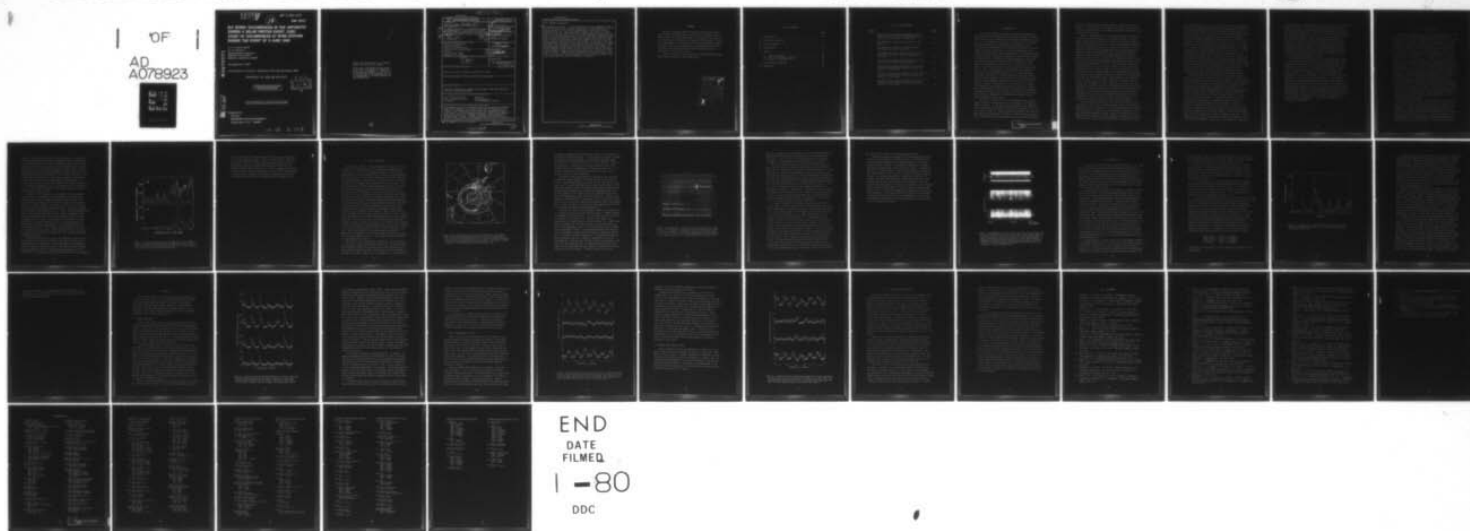
UNCLASSIFIED

SU-SEL-79-005

DNA-4911F

NL

OF
AD
A078923



LEVEL 10

AD-E 300 634

DNA 4911F

ELF SPHERIC OCCURRENCES IN THE ANTARCTIC DURING A SOLAR PROTON EVENT: CASE STUDY OF OCCURRENCES AT BYRD STATION DURING THE EVENT OF 9 JUNE 1968

A. C. Frazier-Smith
R. A. Helliwell
Radioscience Laboratory
Stanford University
Stanford, California 94305

19 September 1979

Final Report for Period 1 December 1977-30 November 1978

CONTRACT No. DNA 001-78-C-0117

APPROVED FOR PUBLIC RELEASE;
DISTRIBUTION UNLIMITED.

DDC
REFILED
JAN 8 1980
E

THIS WORK SPONSORED BY THE DEFENSE NUCLEAR AGENCY
UNDER RDT&E RMSS CODE B322078462 I25AAXHX63349 H2590D.

Prepared for
Director
DEFENSE NUCLEAR AGENCY
Washington, D. C. 20305

79 22 5 012

AD A 0 78923

DDC FILE COPY

62710H

Destroy this report when it is no longer needed. Do not return to sender.

PLEASE NOTIFY THE DEFENSE NUCLEAR AGENCY,
ATTN: STTI, WASHINGTON, D.C. 20305, IF
YOUR ADDRESS IS INCORRECT, IF YOU WISH TO
BE DELETED FROM THE DISTRIBUTION LIST, OR
IF THE ADDRESSEE IS NO LONGER EMPLOYED BY
YOUR ORGANIZATION.



18 DNA, S'BLE

UNCLASSIFIED

SECURITY CLASSIFICATION OF THIS PAGE (When Data Entered)

19 REPORT DOCUMENTATION PAGE		READ INSTRUCTIONS BEFORE COMPLETING FORM
1. REPORT NUMBER DNA 4911F, AD-E300 634	2. GOVT ACCESSION NO.	3. REPORT'S CATALOG NUMBER 9
4. TITLE (and Subtitle) ELF SPHERIC OCCURRENCES IN THE ANTARCTIC DURING A SOLAR PROTON EVENT: CASE STUDY OF OCCURRENCES AT BYRD STATION DURING THE EVENT OF 9 JUNE 1968		5. TYPE OF REPORT & PERIOD COVERED Final Report for Period 71 Dec 77-30 Nov 78
6. AUTHOR(s) A. C. Fraser-Smith R. A. Helliwell	14	7. PERFORMING ORG. REPORT NUMBER SEL-79-005
9. PERFORMING ORGANIZATION NAME AND ADDRESS Radioscience Laboratory Stanford University Stanford, California 94305	15	8. CONTRACT OR GRANT NUMBER(s) DNA 001-78-C-0117
11. CONTROLLING OFFICE NAME AND ADDRESS Director Defense Nuclear Agency Washington, D.C. 20305	11	10. PROGRAM ELEMENT, PROJECT, TASK AREA & WORK UNIT NUMBERS Subtask I25AAXH633-49
14. MONITORING AGENCY NAME & ADDRESS (if different from Controlling Office) 12 45		12. REPORT DATE 19 September 1979
		13. NUMBER OF PAGES 46
		15. SECURITY CLASS (of this report) UNCLASSIFIED
		15a. DECLASSIFICATION/DOWNGRADING SCHEDULE 17 X633
16. DISTRIBUTION STATEMENT (of this Report) Approved for public release; distribution unlimited.		
17. DISTRIBUTION STATEMENT (of the abstract entered in Block 20, if different from Report)		
18. SUPPLEMENTARY NOTES This work sponsored by the Defense Nuclear Agency under RDT&E RMSS Code B322078462 I25AAXHX63349 H2590D.		
19. KEY WORDS (Continue on reverse side if necessary and identify by block number) Solar Proton Event (SPE) Antarctica Polar Cap Absorption (PCA) Sanguine/Seafarer ELF Sferics Pc 3 Geomagnetic Pulsations		
20. ABSTRACT (Continue on reverse side if necessary and identify by block number) Electromagnetic waves with frequencies above the extremely-low-frequency range (ELF; frequencies in the range 5 Hz-3 kHz) are susceptible to a variety of solar proton event (SPE) effects when propagating through a polar region in the earth-ionosphere waveguide. These effects appear to become less severe as the frequency of the waves becomes smaller and approaches the ELF range. Although measurements have been lacking, it would be expected that ELF wave propagation through the polar regions would		

DD FORM 1 JAN 73 1473 EDITION OF 1 NOV 65 IS OBSOLETE

UNCLASSIFIED

SECURITY CLASSIFICATION OF THIS PAGE (When Data Entered)

332400

18

UNCLASSIFIED

SECURITY CLASSIFICATION OF THIS PAGE(When Data Entered)

20. ABSTRACT (Continued)

be comparatively stable. To investigate polar ELF wave propagation during an SPE, we have carried out a series of measurements of the properties of ELF sferics (75 Hz) at a polar location (Byrd Station, Antarctica) during a moderately-large SPE. These measurements suggest that an SPE can significantly alter the characteristics of ELF signals propagating through the polar regions: during the first 24 hours of the SPE there was a reduction of about 50% in the median amplitudes of the sferics, compared with their amplitudes before the SPE, and there were substantial changes in their rates of occurrence. However, there was no polar cap 'blackout' of the sferics, and their amplitude reduction appeared to be no greater than the reductions occasionally observed at lower latitudes in experiments with man-made ELF signals. Thus our measurements provide support for the view that ELF signal propagation through the polar regions during an SPE is comparatively stable. At frequencies below the ELF range, we note the appearance of Pc 3 pulsations at the start of the SPE. Further study of the possible stimulation of these pulsations by SPE's and additional measurements of the SPE-related changes of ELF spheric characteristics at polar locations are desirable.

UNCLASSIFIED

SECURITY CLASSIFICATION OF THIS PAGE(When Data Entered)

PREFACE

We wish to thank the 1968 Byrd Station "wintering-over" team, Steven Andrews and Robert Raney, for their care in obtaining the ELF data on which this research was based. The important role played by John Katsufakis in organizing the Antarctic field operation is gratefully acknowledged. We would also like to thank Frank Soong, Jerry Yarbrough, Kevin Gillette, Paula Renfro, and Frank Orabona for their assistance with the data processing, and William Moler and Carl Greifinger for helpful discussions.

Support for this work was provided by the Defense Nuclear Agency, RAAE, through Contract No. DNA 001-78-C-0117.

Accession For	
NTIS GRA&I	<input checked="checked" type="checkbox"/>
DDC TAB	<input type="checkbox"/>
Unannounced	<input type="checkbox"/>
Justification	
By _____	
Distribution/	
Availability Codes	
Dist	Availand/or special
A	

TABLE OF CONTENTS

	<u>Page</u>
I. INTRODUCTION - - - - -	5
II. THE SPE OF 9 JUNE 1968 - - - - -	9
III. BYRD STATION DATA- - - - -	13
IV. DATA ANALYSIS- - - - -	20
V. RESULTS- - - - -	25
V.1 Sferic Amplitudes - - - - -	25
V.2 Rate of Occurrence of Sferics - - - - -	28
V.3 Average Time between Sferics- - - - -	30
VI. DISCUSSION AND CONCLUSION- - - - -	32
VII. REFERENCES - - - - -	34

LIST OF ILLUSTRATIONS

<u>Figure</u>		<u>Page</u>
1	Variation of the three-hour geomagnetic activity index ap and of the auroral electrojet activity index AE for the interval 5-13 June 1968 - - - - -	11
2	Map showing the location of Byrd Station in the Antarctic- - - - -	14
3	Reproduction of a section of the Byrd Station strip chart record for 9 June 1968 - - - - -	16
4	Spectrograms of ELF/VLF sferic activity at Byrd Station (BY) during one synoptic minute on 10 June 1968- - - - -	19
5	An example of the amplitude fluctuations of 75 Hz sferic activity observed at Byrd Station - - - - -	22
6	Variation of the median amplitude of 75 Hz sferics observed at Byrd Station, Antarctica, during the interval 7-12 June 1968- - - - -	26
7	Variation of the rate of occurrence of 75 Hz sferics observed at Byrd Station, Antarctica, during the interval 7-12 June 1968- - - - -	29
8	Variation of the average time between 75 Hz sferics observed at Byrd Station, Antarctica, during the interval 7-12 June 1968- - - - -	31

I. INTRODUCTION

For over two decades it has been known that the attenuation of electromagnetic waves propagating in the earth-ionosphere waveguide is particularly low for frequencies less than 300 Hz (References 1, and 2), i.e., for frequencies in the lowest ten percent of the extremely-low-frequency band (ELF; frequencies in the range 5 Hz-3 kHz). Further, because these waves are reflected from the base of the ionosphere, with little penetration, it would be expected that their propagation would be more stable during natural or man-made ionospheric disturbances than the waveguide propagation of higher frequency waves. For these reasons, and because the lower-frequency ELF signals can reach depths in the sea on the order of 100 m before the signals become too attenuated for reception (the skin depth for a 100 Hz signal in the sea is about 25 m), there has been an interest within the U.S. Navy in the possible use of ELF signals for worldwide communication with submerged receivers from a single land-based transmitter (Reference 3). Research sponsored by the Navy on the generation and propagation of ELF signals has been conducted largely under the names 'Sanguine' (References 4, 5, 6, and 7) and, more recently, 'Seafarer' (Reference 8). As a result of this research, our knowledge of the properties of naturally occurring ELF signals and of the propagation characteristics of man-made ELF transmissions (predominantly from the Navy's Wisconsin Test Facility described by White and Willim [Reference 9] and Bannister [Reference 10]) has greatly expanded in recent years.

The temporal stability of ELF signal propagation over large distances was one of the important issues studied during the Sanguine/Seafarer projects. It was found that the propagation was indeed very stable, despite some variability at night (e.g., References 9, 10, 11, 12, 13, 14, 15, and 16). However, because the Wisconsin Test Facility only became fully operational in 1971, just after the maximum phase of the last sunspot cycle, the measurements were of necessity made almost

entirely at times that were relatively quiet in terms of ionospheric behavior. In particular, no measurements were made of the effects of a solar proton event (SPE) on ELF signal propagation along paths passing through the polar regions.

There are several reasons why ELF signal propagation through the polar regions could be expected to be affected by an SPE. The most general reason follows from the observation of SPE-related changes at frequencies above the ELF range: it is well-known that electromagnetic waves with frequencies above the ELF range are susceptible to a wide variety of SPE effects when propagating either directly through the polar ionosphere or through a polar region in the earth-ionosphere waveguide. These effects include intense absorption, now known as polar-cap absorption (PCA), for waves with frequencies in the HF (3-30 MHz) and lower VHF (30-300 MHz) bands, and phase and amplitude changes for waves with frequencies in the VLF (3-30 kHz) and LF (30-300 kHz) bands (References 17, 18, 19, and 20). Because of their proximity in frequency to the ELF range, and their stability of propagation (which has led to the use of these frequencies for communication, navigation, and precise time and frequency comparisons over global distances [Reference 20]), the SPE-induced changes in the propagation characteristics of the VLF waves are of particular significance. Studies of these changes, and the changes at higher frequencies, have shown that they are caused by the large increases of ionization produced by SPE's below the normal D-region base of each polar ionosphere (e.g., Reference 21). Thus there is a more specific reason to expect an SPE effect at ELF: the characteristics of the earth-ionosphere waveguide for ELF wave propagation in the polar regions during an SPE are altered, just as they are altered for VLF and higher-frequency wave propagation.

Crain and Booker (Reference 22) were the first to point out the important role of the ions in these anomalous regions of ionization in affecting VLF and LF transmission. In an important theoretical analysis, Field (Reference 23) showed that the propagation of ELF waves in the earth-ionosphere waveguide could be strongly influenced by the ionic component of the anomalous D-region ionization produced during an SPE. In a discussion of this work, Wait (Reference 8) comments that "under

such PCA conditions ions are really controlling the [ELF] propagation." Although experimental measurements of ELF wave propagation through the polar regions during an SPE are lacking, anomalous enhancements of D-region ionization similar to those occurring in the polar regions during an SPE are produced on occasion by the precipitation of energetic electrons, and these enhancements have been shown to cause ELF signal propagation anomalies (References 13, 14, 15, 16, and 24). (Similar effects have also been observed at VLF [Reference 25].) It is particularly relevant to the present study that these anomalies in ELF signal propagation do not always degrade the quality of the signal: both the experimental measurements and the results of computations using a waveguide model computer program (References 24, and 26) indicate that the strength of the ELF signals may be either increased or decreased, depending on (1) the location of the propagation paths relative to the regions of charged particle precipitation and (2) on the spatial extent and composition of the resulting ionization. Nevertheless, it is worthwhile noting that the majority of the propagation anomalies reported to date have involved a reduction in ELF signal strength.

Although the Wisconsin Test Facility was not operating during the last solar maximum, there were research stations in the Antarctic making recordings of naturally occurring ELF signals, and it is possible to obtain information about SPE effects at ELF in the polar regions by analyzing these recorded data. The purpose of this report is to present results obtained from measurements on naturally occurring ELF sferics recorded at Byrd Station, Antarctica, during a moderately large SPE. The results are limited by several factors. First the sferic observations were made at a single station, and it has been recognized for some time (e.g., Reference 2) that multi-station observations can provide more definitive information (since it is possible to determine the location of the sferics). Second, the SPE occurred in the middle of the austral winter, when the entire southern polar cap ionosphere was in constant darkness. Our results are therefore only strictly applicable to these ionospheric conditions. Finally, there was a limitation on the quantity of data we could process, and a full statistical analysis of many days or even months of sferic data

to determine their undisturbed characteristics in detail was outside the scope of this effort. Because of this statistical limitation, our results are indicative and not definitive. Despite these limitations, our measurements appear to be the first of their kind, and they provide new information about SPE effects on ELF sferics at a polar location, and they indicate that ELF signal propagation through the polar regions can be affected significantly by the occurrence of an SPE. Our case study suggests that the signal strength is more likely to be degraded than to be enhanced, but further measurements using a controlled source and multi-station observations during the upcoming solar maximum phase are desirable to determine the general form of the SPE-induced ELF propagation anomalies.

To conclude this introduction, we note that we have been unable to find a specific definition of the term 'solar proton event,' even though a classification system has been introduced for these events (Reference 27) and the term is used extensively in the literature. Further, the abbreviation SPE is sometimes used to denote 'solar particle event' (e.g., Reference 21), which is not necessarily synonymous with 'solar proton event.' Possible confusion may also be caused by the term 'polar-cap absorption event' or, equivalently, 'PCA event,' which preceded the other terms historically and which is often used alternatively with solar proton event (as pointed out by Hultqvist [Reference 28]). We will use solar proton event to denote the terrestrial atmospheric effects produced by a solar proton flare (References 29, and 30). These terrestrial effects include the production of anomalous ionization in the ionospheric D-region, which in turn causes polar-cap absorption. Thus PCA will be used in its original restricted sense.

II. THE SPE OF 9 JUNE 1968

At 0830 UT on 9 June 1968, a flare with an importance in the range 2N to 4B (classified as 3B by Švestka and Simon [Reference 31]) commenced on the southern hemisphere (S14, W08) of the sun and initiated a number of interplanetary and terrestrial phenomena before it ended near 1120 UT. Less than two hours after the start of the flare, the earth-orbiting Explorer 34 satellite detected substantial increases in solar proton intensities in the energy ranges $E_p \geq 10$ MeV, $E_p \geq 30$ MeV, and $E_p \geq 60$ MeV (Reference 32). The durations of the increases varied with the proton energies: over 24 hours for the $E_p \geq 60$ MeV range, and until 12 June for the $E_p \geq 10$ MeV range. Other satellite measurements and one balloon measurement of the energetic particles produced by the flare are tabulated in summarized form by Švestka and Simon (Reference 31). Large-scale terrestrial changes commenced with the arrival of these solar protons in the earth's upper atmosphere. In particular, a PCA event began at approximately 1000 UT (Reference 31). Measurements by Masley and Satterblom (Reference 33) with riometers at the two magnetically conjugate polar stations McMurdo Sound, Antarctica, and Shepard Bay, N.W.T., Canada, gave a maximum absorption of 6.0 db at 30 MHz. By this measure, the PCA event was the seventh largest of the 31 events with at least 1 db of observed daytime 30 MHz riometer absorption tabulated by Zmuda and Potemra (Reference 20) for the 1965-1969 solar maximum period. Švestka and Simon (Reference 31), using the SPE notation of Smart and Shea (Reference 27), list an importance of 230 for the event.

Geomagnetic storms generally form a component of the terrestrial effects comprising an SPE, even though they are not caused by the energetic (10-100 MeV) protons that produce the most characteristic SPE effects. Instead, the SPE-associated geomagnetic storms are caused by the bursts of solar plasma that are emitted from the active regions containing the proton flares. Because the energies of the charged particles in the plasma are low (the proton energies are typically less than 1 keV), the bursts of plasma take considerably

longer to reach the earth than the 10-100 MeV protons. In the case of the 9 June 1968 SPE event, the major geomagnetic storm that formed part of the event started with a sudden commencement at 2154 UT on 10 June. There was therefore a delay of about 36 hours between the start of the SPE and the start of its component geomagnetic storm. Figure 1 shows the variation of the three-hour geomagnetic activity index a_p and of the auroral electrojet activity index AE for the interval 5-13 June. It is interesting to note that the AE index began to respond to the SPE over 24 hours before there was any large response of the a_p index. The latter index reached its greatest amplitude in the interval 03-06 UT on 11 June, and the geomagnetic storm, as measured by a_p (or, equivalently, by the Kp index), was the largest in the one year interval 1 October 1967 through 30 September 1968.

As noted in the introduction, no measurements of the propagation characteristics of man-made ELF signals through a polar region are available for this SPE. However, measurements made in Hawaii of the phase differences between the 10.2 kHz (VLF) transmissions from Omega stations in Norway and Hawaii showed that by 1100 UT on 9 June the SPE was affecting the Norway-Hawaii propagation path, which passes through the north polar region (Reference 34; W. F. Moler, Personal communication, 1978). The maximum disturbance of the VLF signals propagating along this path occurred during 11 June, and the effects of the SPE finally disappeared late on 13 June. Švestka and Simon (Reference 31) report that the PCA reached a maximum near 08 UT on 10 June and thereafter declined until it became unmeasurable on 12 June (the duration of the PCA was about 63 hours). The difference in the duration of the SPE is consistent with the observation by Reid (Reference 19) that PCA effects on long-distant VLF circuits are generally of much longer duration than the absorption effects.

At the time of occurrence of the 9 June 1968 SPE, synoptic ELF/VLF measurements were being made routinely at Byrd Station, Antarctica, by Stanford University researchers. These measurements were intended for studies of naturally occurring signals in the upper ELF and VLF ranges, and the frequency response of the recording system began to drop off below 100 Hz. Thus there was a possibility that the synoptic measurements

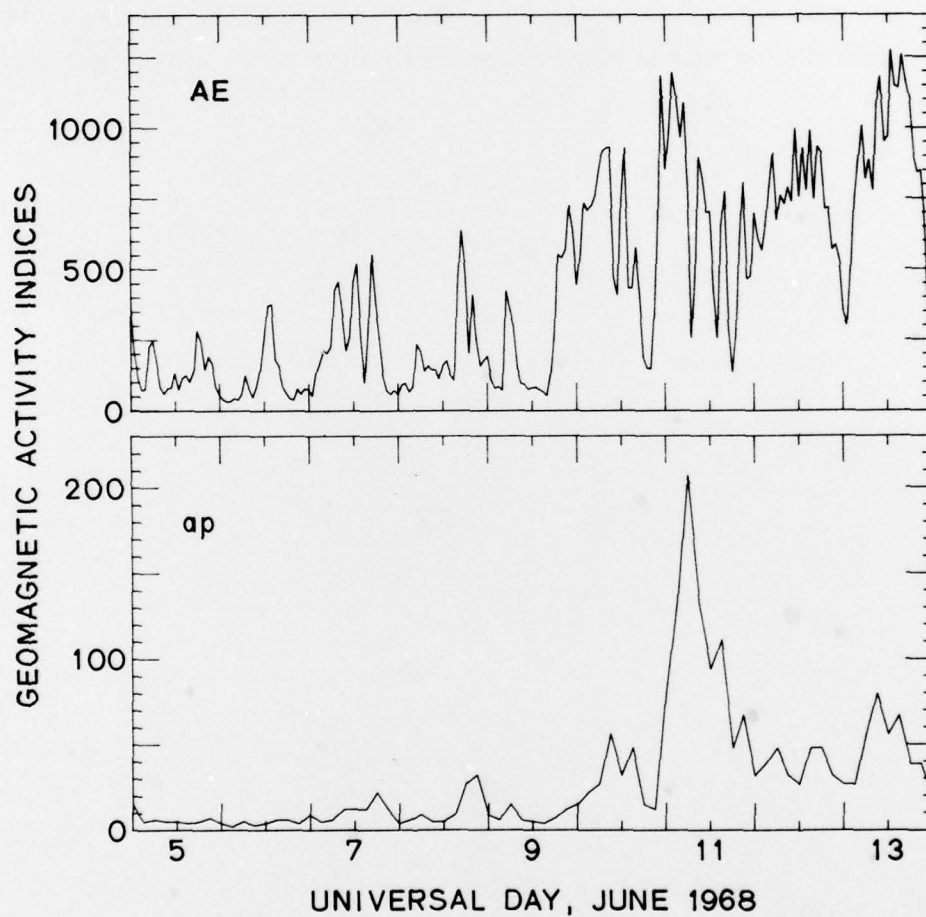


Figure 1. Variation of the three-hour geomagnetic activity index ap and of the auroral electrojet activity index AE for the interval 5-13 June 1968. The SPE started before 1200 UT on 9 June, although this is not evident in the activity indices.

could not be used to study SPE effects on ELF signals with frequencies in the Sanguine/Seafarer range. However, for this one SPE, continuous recordings of natural ELF signals were also being made by using an exceptionally long (33.5 km) dipole antenna and a system with good frequency response down to about 10 Hz. Since it appeared that adequate ELF data would be available, we undertook a case study of the properties of the ELF sferics occurring at Byrd Station during the course of the 9 June 1968 SPE, with the results reported in the following sections.

III. BYRD STATION DATA

Byrd Station (79.98°S, 120.02°W; geomagnetic latitude 70.4°S; see Figure 2) was established during the International Geophysical Year (1957-1958) as a facility for geophysical research in the Antarctic, and Stanford University operated ELF/VLF receivers and other geophysical measuring apparatus at this station throughout the interval 1958-1971. The research programs varied from year to year, but they consistently included synoptic magnetic tape recordings of ELF/VLF activity. The most common format for these analog recordings, and the one relevant to the present study, was to record four one-minute intervals of activity each hour, starting at 5, 20, 35, and 50 minutes after the start of the UT hour. During the initial few seconds of each of these one-minute intervals, a known 5 kHz amplitude calibration signal was injected into the system. Three loop antennas were buried beneath the snow surface and were used to measure the north-south (N-S), east-west (E-W), and vertical (V) magnetic components of the ELF/VLF signals. In addition, a vertical whip antenna was available to measure the vertical electric component of the signals. However, not all these signal components were recorded on magnetic tape at all times. During the 9 June 1968 SPE, only the N-S loop antenna was used for the synoptic recordings. Thus, for this event, the recording system had maximum response to ELF/VLF signals travelling in a N-S direction (or S-N direction) and no response to signals travelling in an E-W (or W-E) direction. It should also be pointed out that the N-S line was determined by compass. Thus the horizontal N-S and E-W directions were neither geographic nor geomagnetic, but were determined instead by the location of the southern magnetic dip pole. We will describe these directions as being magnetic N-S and E-W.

Data acquisition at Byrd Station included the routine collection of analog data on eight-channel paper strip charts. The format of the chart recordings varied; at the time of the 9 June 1968 SPE the first four channels recorded the output signals from (1) an H-field magnetometer, (2) a 30-MHz riometer, (3) a Y-component (i.e., geographic E-W)

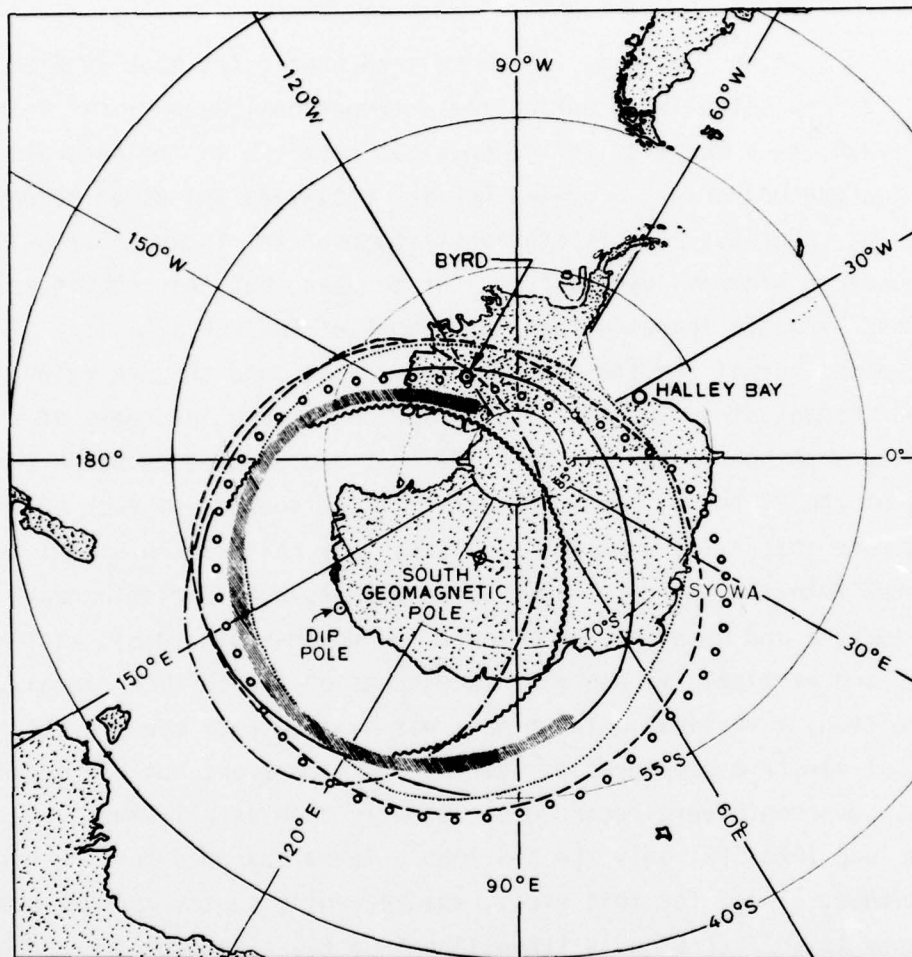


Figure 2. Map showing the location of Byrd Station in the Antarctic. Also shown are the approximate locations of the south geomagnetic pole and the dip (or magnetic) pole. The hatched, dashed, and dotted lines outline the location of the auroral zone. The figure is based on Figure 1 of Morozumi and Helliwell (Reference 35).

ULF magnetic pulsation sensor (0.02-5 Hz), and (4) HF hiss detectors at 0.5 MHz and 4.9 MHz (two traces). The remaining four channels recorded the integrated signal amplitudes in the following frequency bands: (5) 61-75 kHz (LF), (6) 31-38 kHz (LF), (7) 11-13 kHz (VLF), and (8) 1-2 kHz (upper ELF). Time marks on the charts enabled the time of any distinct feature to be determined to an accuracy of about ± 10 s. As a relevant illustration of the form of these data, Figure 3 shows a section of the chart for 9 June 1968.

Inspection of the chart records for the interval 8-15 June 1968 confirmed the general features of the SPE outlined in the previous section. One difference was a start time of 1215 ± 0005 UT on 9 June (see Figure 3) for the Byrd PCA, which is later than the 1000 UT (time accurate to within an hour) listed by Švestka and Simon (Reference 31). Reid and Sauer (Reference 36) observed the simultaneous onset of PCA at Byrd (southern auroral zone), South Pole (geographic south pole), and Vostok (geomagnetic south pole) during the SPE of 5 February 1965. However, such simultaneity is exceptional, and it is usual for a delay of an hour or more to occur between the observation near the geomagnetic pole of the first stage of a PCA event and the sudden extension of the PCA to auroral and lower latitudes (Reference 28).

There was an interesting correspondence (within the uncertainty of ± 5 m) between the start of the PCA and the start of a lengthy interval of geomagnetic pulsation activity. The pulsations could be classified as belonging to the category Pc 3 (periods in the range 10-45 s), because they were regular and had a period of about 35 s. Later, these pulsations become very large and irregular, particularly after the start of the geomagnetic storm on 10 June, which was clearly recorded on the magnetometer channel. A correspondence between the start of a burst of geomagnetic pulsations and the onset of riometer absorption was first noted by Morozumi (Reference 37) in data from Byrd Station; the correspondence was later studied in greater detail by Chivers (Reference 38), using data from the more northerly Siple Station. However, there are different forms of riometer absorption and no link appears to have been made previously between PCA specifically and the occurrence of Pc 3 pulsations. If there is such a link, as our

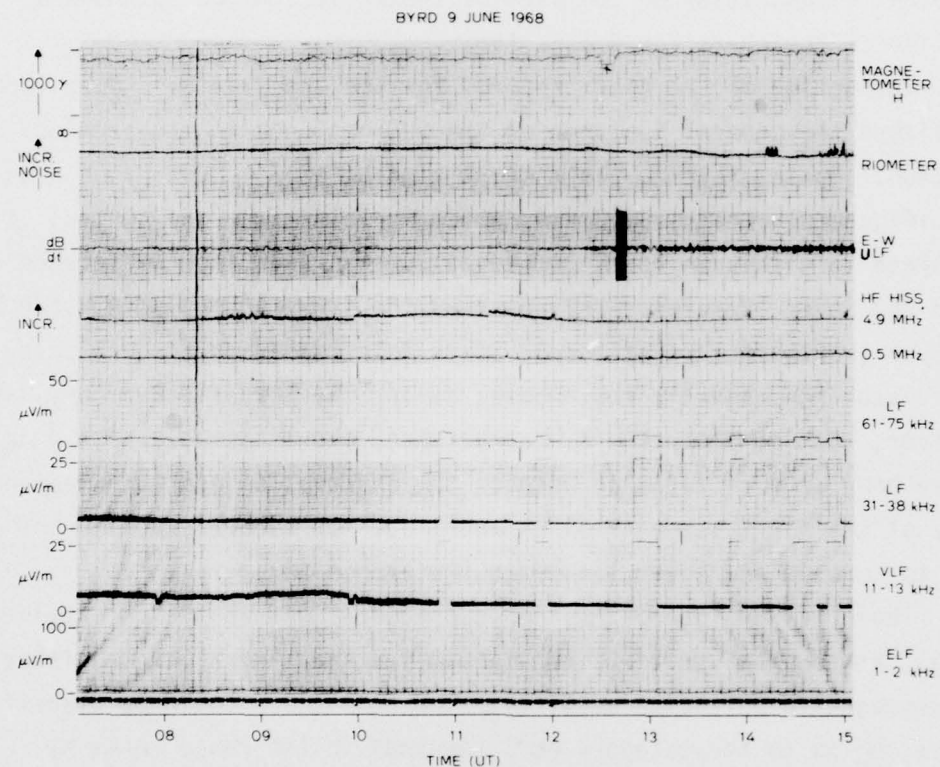


Figure 3. Reproduction of a section of the Byrd Station strip chart record for 9 June 1968. The large signal occurring at about 1240 UT in the ULF channel is produced by the ULF calibration system. A cross next to a small dip in the magnetometer trace was inserted by the station operators to indicate that the dip is artificial.

observation suggests, it could provide a test of the present theory of generation of the pulsations (see Reference 39 for a description of this theory), since an influx of 10-100 MeV protons into the lower ionosphere is a particularly well defined source of stimulation.

The Byrd riometer recorded two maximums of absorption on 10 June 1968: one, the smaller, occurred at about 0530 UT and the other at about 1300 UT. The riometer was even more strongly affected on 11 June, during the main phase of the geomagnetic storm. Particularly strong absorption was recorded during the intervals 0330-0430 UT and 1400-1900 UT on this day, during which times very large and irregular geomagnetic pulsations were also observed. The riometer thereafter began to recover, but it did not finally return to its initial quiet level until 15 June. The activity recorded on the other radio channels appeared to be affected by the SPE for a shorter time. Following the start of the SPE, the signals in each of the ELF, VLF, LF, and HF channels dropped either to zero or to low levels and remained there until 11 June, when some activity reappeared in these channels, and there was a large burst in the 1-2 kHz channel during the interval 1400-2000 UT.

An unusual feature of the equipment at Byrd Station during the austral winters of 1967-1969 was a VLF transmitting antenna consisting of two exceptionally long horizontal dipoles. One of these dipoles was 33.5 km long and was aligned in the magnetic N-S direction; the other, 17 km long, was perpendicular to it. More complete details of the antenna are given by Siren (Reference 40). The antenna was used primarily to send VLF signals in various modes of elliptical polarization to satellites passing over the station. However, it was also possible to use the dipoles as receiving antennas, and in each of the winters of 1967-1969 the 33.5 dipole was used for a series of "longwire" recordings of natural ELF/VLF activity. These recordings were distinguished from the synoptic recordings primarily by the fact that they were continuous. Their frequency response was also superior below 100 Hz: the longwire recordings covered frequencies down to about 10 Hz, whereas the synoptic recordings were not intended to give information below about 100 Hz. At the time this study was undertaken it was unclear whether the synoptic recordings could be used to study

SPE effects on ELF signals with frequencies below 100 Hz.

Since both synoptic and longwire ELF/VLF recordings were available for the 9 June 1968 SPE, frequency displays of overlapping intervals of data were prepared and the frequency responses of the two recording systems compared. The comparison showed that the synoptic data gave information about sferic occurrences down to a frequency of about 40 Hz. Figure 4 shows an example of this comparison, together with some typical ELF sferic activity. Because the synoptic data were already in a convenient sampled form (one minute of data every 15 minutes), and each sample contained a known calibration signal that could be used to check the stability of the recording system (the longwire recordings were not calibrated), we decided to use the synoptic data to investigate the behavior of the ELF sferics recorded at Byrd during the SPE. A choice of frequencies was required; we chose 75 Hz, since frequencies in the range 70-80 Hz are often used in experiments involving the Wisconsin Test Facility and frequencies in this range can probably be considered to be prime candidates for use in a larger-scale ELF communication system.

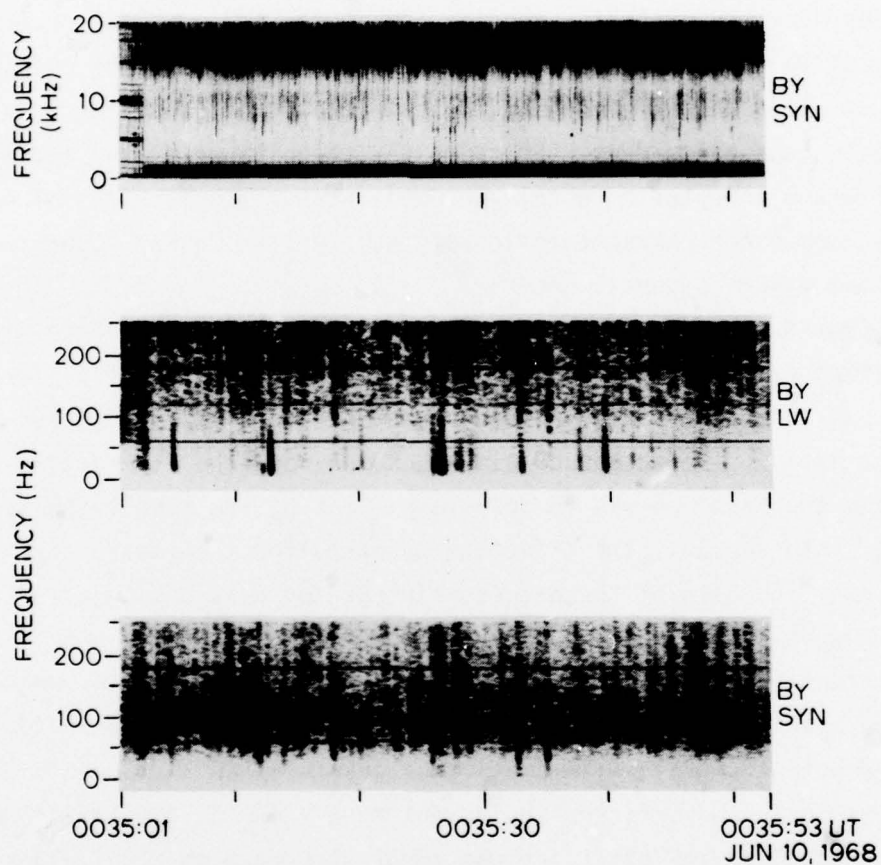


Figure 4. Spectrograms of ELF/VLF sferic activity at Byrd Station (BY) during one synoptic minute on 10 June 1968. The top panel shows the overall activity in the range 0-20 kHz, and the two bottom panels show a more detailed view of the activity in the range 0-250 Hz, as recorded on the longwire (LW) antenna and on the regular synoptic (SYN) loop antenna. The band of minimum activity at 12 kHz in the top panel is an instrumental effect.

IV. DATA ANALYSIS

The Byrd Station ELF/VLF synoptic data were analyzed in two stages. First, the original analog data were converted to digital form by playing back the magnetic tapes at four times the original recording speed of 15 ips, filtering, detecting, and integrating the output, and then sampling and re-recording the data (now in digital form) on magnetic tape cartridges. Next the digital data were analyzed with an XDS Sigma 5 computer to obtain the median amplitudes, rates of occurrence, and other characteristics of the sferics (75 Hz) occurring in each one minute synoptic interval.

Considering the first stage of this analysis, a bandpass filter-amplifier was used to select the frequency passband for the sferics; its upper and lower cut-off frequencies were set at 310 and 290 Hz, respectively. The passband gain was 20 db, and the attenuation rate outside the passband was 48 db/octave. Taking the tape speed-up factor into account, the effective passband for the sferics was 72.5-77.5 Hz. The gain of the detector-integrator unit was adjusted to give output sferic amplitudes predominantly in the range 0-5 V, as required for input to the digitizer (input voltages in the range -5 to +5 V were specified). Occasional very large sferics would produce integrated output signals with amplitudes greater than 5 V; such signals were assigned an amplitude equivalent to 5 V during digitization. The input signal to the digitizer was sampled every 3 ms (equivalent to 12 ms in real time), and the A/D conversion resolution was 12 bits, i.e., the 0-5 V range of the input signal amplitudes was subdivided into 2048 amplitude units. In the following, when we refer to the relative amplitude of a sferic, we use the digital amplitude scale of 0-2048 amplitude units.

Although emphasis is given in this work to the temporal changes in the measured characteristics of the sferics, and no absolute measure of the sferic amplitudes (i.e., their apparent field strengths) is required, it is possible to derive an approximate absolute amplitude measure for the sferics from the calibration signals recorded on the

original magnetic tapes. When the conversion factor is calculated for our relative amplitude scale, we find that 1000 of our digital amplitude units correspond approximately to a field strength of 2 mV/m.

Figure 5 shows a plot of a representative interval of digitized ELF sferic data. The antenna and recording system were not coupled during the initial second of this plot, but the ELF data are included to give an indication of the internal system noise. Numerous sferics can be seen in the following 5-second interval, including a large burst starting just after 2.0 s.

To ensure uniformity in the digital data, the original magnetic tapes were played back and the analog data digitized in one session without intermediate changes in the gain settings. In addition, the 5 kHz calibration signal amplitudes were monitored on strip chart recordings during the digitization session: the amplitudes remained constant to within a measurement accuracy of $\pm 0.7\%$.

In the second stage, following digitization, the data were processed by computer to obtain the amplitude and occurrence characteristics of the sferics. Before commencing this processing, however, we adopted an operational criterion to distinguish sferics of different amplitudes. In using this criterion, we first divided the sferics into three categories according to whether successive samples had (1) one or more increases of amplitude followed by one or more decreases, (2) two or more increases of amplitude followed by two or more decreases, and (3) three or more increases followed by three or more decreases. Two additional categories were then created by removing the sferics in category 2 from those in 1 (category 4) and by removing the sferics in category 3 from those in 2 (category 5). The sferics could then be divided into three size groups and one inclusive group as follows:

small sferics:	sferics in category 4
medium sferics:	sferics in category 5
large sferics:	sferics in category 3
all sferics:	sferics in category 1

This system of classification is used throughout the remainder of this communication.

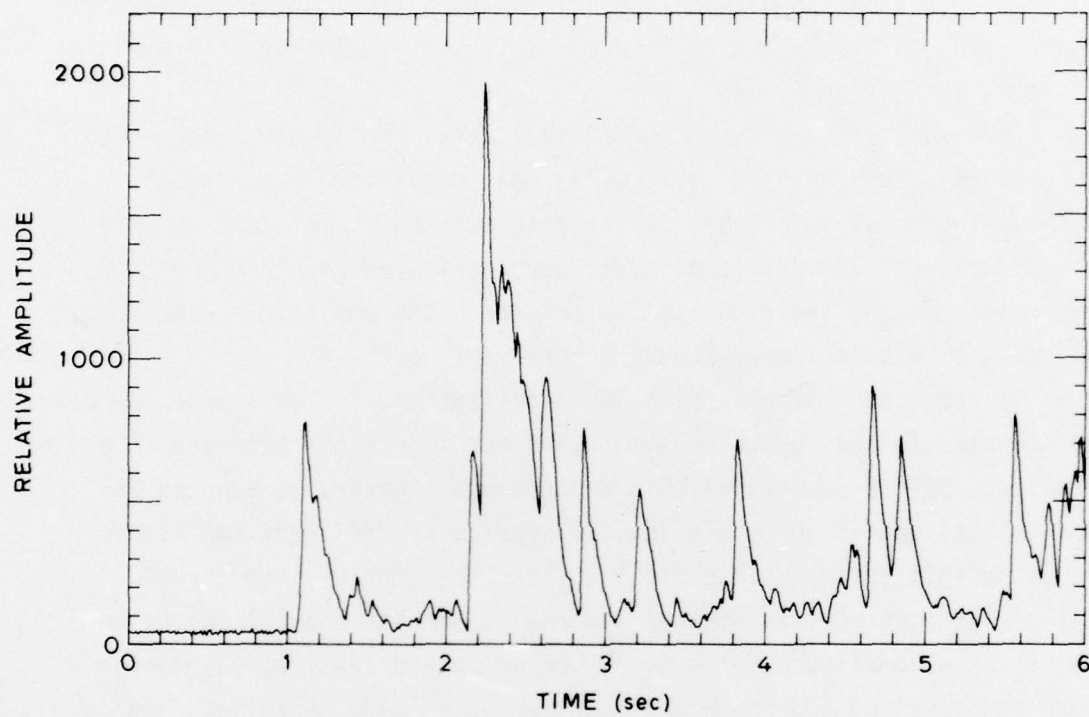


Figure 5. An example of the amplitude fluctuations of 75 Hz sferic activity observed at Byrd Station. The first 1 second of data represents system noise.

Once the sferics in a particular interval of data were divided into their different categories, it was possible to compute their average amplitudes, rates of occurrence, times between occurrences, and other statistical data. Because of the synoptic form of the ELF data, it was convenient to treat each one-minute interval of sferic data as a unit. The total number of sferics occurring in these one-minute intervals was variable, but during the period of six days chosen for this SPE study there were never less than 600. Even in the individual category with the smallest number of occurrences (medium sferics), there were never less than 100 sferics in a one-minute interval. Thus the statistical data derived for these one-minute intervals should be based on an adequate number of sferics.

Because of the artificial upper limit imposed on the amplitudes of the sferics by our digitization process (exceptionally large sferics could also possibly be limited in amplitude by the finite response of the original recording system), we computed the median amplitude of the sferics in each size category in preference to the average amplitude. However, due to computer storage limitations, we were not always able to compute the median amplitude for all the sferics in a one-minute interval. We therefore adopted a hybrid approach: the interval of data was divided into four equal parts, and the median amplitudes computed for the sferics in each part; the four median amplitudes were then averaged to obtain an overall (average) median for the interval.

In addition to computing median amplitudes, we also computed the rate of occurrence of the sferics, and the time interval between sferics, for each size category and for all sferics in the one-minute intervals. The interval chosen for this computer analysis was 7-12 June 1968. Thus for each class of sferics there were in principle 96 intervals for which amplitude and occurrence data were obtained each day, and 576 measurements of each variable were made over the six-day period. In practice, the longwire antenna was being used for VLF transmissions during some of the intervals, or the recording system was not in operation, and useful sferic data were not obtained. There were 87 such intervals during the six-day period, or about 15% of the total. This was a significant percentage of outages, but as shown in

the following section, the remaining data were sufficient to give a complete picture of the variation of spheric amplitudes and occurrences at Byrd Station during the SPE.

V. RESULTS

The principal results of our data analysis are presented in the form of two figures showing the variation during the 9 June 1968 SPE of the median amplitudes and rates of occurrence of the sferics occurring in the one-minute synoptic intervals. A third figure, showing the variation of the average time between sferics, is also presented. These figures summarize amplitude and time of occurrence measurements on a total of 320,181 sferics.

V.1 SFERIC AMPLITUDES

Figure 6 shows the variation of the median amplitude of the 75 Hz sferics occurring in the one-minute synoptic intervals throughout the period 7-12 June 1968. In this figure, as well as in the two following figures, the top panel shows the variation for all sferics, and the bottom panel shows the individual variations for small (bottom section), medium (middle), and large (top) sferics. The data points apply to each minute of synoptic data, and smooth curves have been drawn through these points by using a computer smoothing algorithm.

Considering the data for all the sferics first, it can be seen that there is a marked reduction in the median amplitudes of the sferics during the first 48 hours of the SPE, as compared with the amplitudes measured during the 56 hours preceding the start of the SPE (i.e., from 0000 UT on 7 June through 0800 UT on 9 June). According to the geomagnetic activity data in Figure 1, there were no geomagnetic disturbances in the four days preceding the 9 June event. Further, although Švestka and Simon (Reference 31) list three instances of satellite detection of energetic proton bursts, there were no detectable energetic charged particle precipitation effects on the ground in the week before the 9 June SPE. Thus the ELF propagation conditions from 0000 UT on 7 June through the commencement of the 9 June SPE appear to be typical of normal, non-SPE, ionospheric conditions.

There are two daily maximums in the median amplitudes of the sferics prior to the start of the SPE. The first of these maximums occurs at

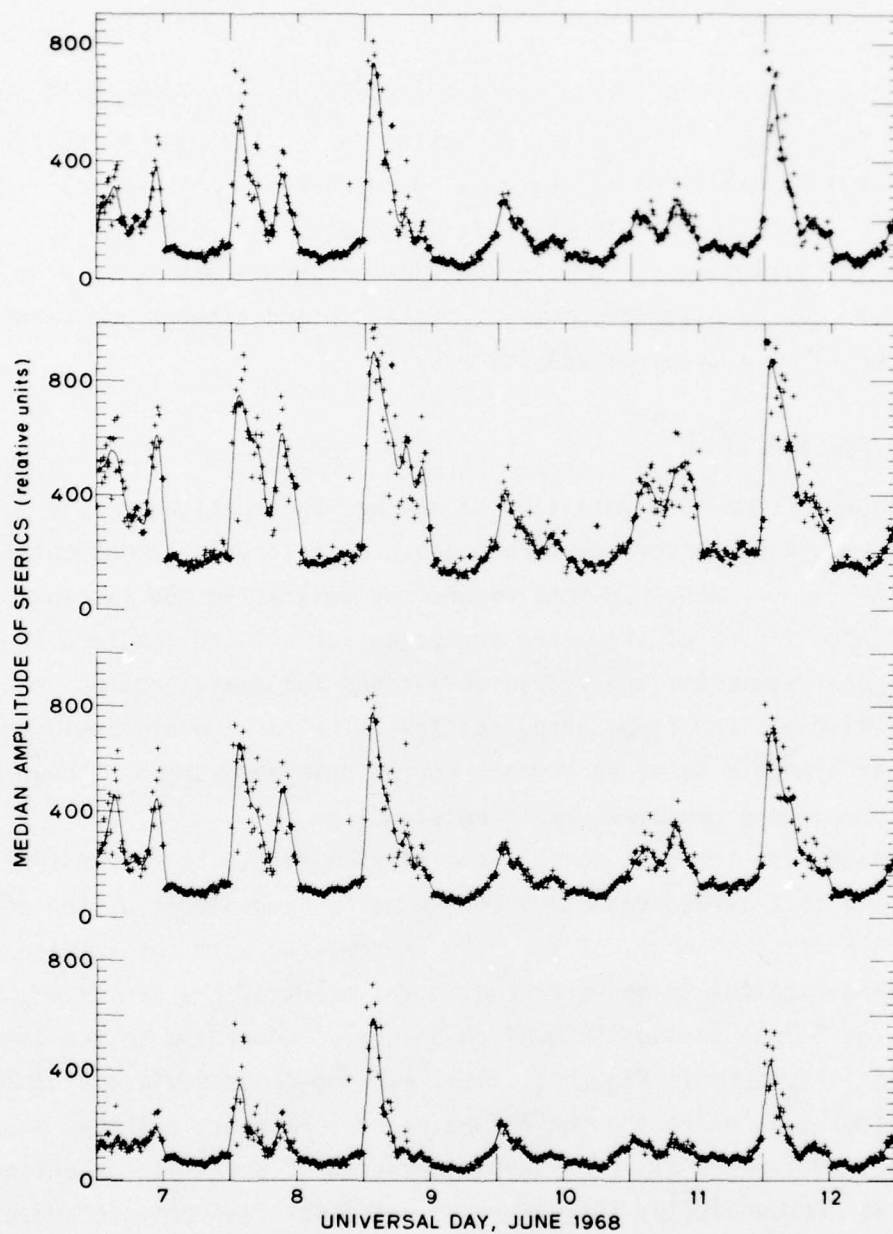


Figure 6. Variation of the median amplitude of 75 Hz sferics observed at Byrd Station, Antarctica, during the interval 7-12 June 1968. The top panel shows data for all sferics; the bottom panel shows data for small (bottom), medium (middle), and large (top) sferics.

about 0100 UT and the other at about 1000 UT. Because our measurements give no information about the location of the sferic sources, we cannot definitely associate these amplitude maximums with particular sferic source regions. However, following Larsen (Reference 41) and using statistics for worldwide thunderstorm activity (Reference 42), we can tentatively associate the maximums with source regions in South-East (S-E) Asia and in the Americas. According to the latter reference, there are three large thunderstorm areas in the world: (1) S-E Asia (the longitude range corresponding to this source region is approximately 90° - 135° E), (2) Africa (15° W- 50° E), and (3) the Americas (45° - 90° W). Sferics from a source region in Africa arrive at Byrd Station from a direction that is roughly magnetic E-W, and thus they are likely to produce only a small response in the ELF/VLF receiver (see Figure 2 and the previous discussion of the Byrd antennas) and can be neglected. The thunderstorm activity in each area has a well-defined diurnal variation; in S-E Asia the activity peaks at about 0800 UT, and in the Americas it peaks at about 2000 UT. The peaks are broad, and there is still much Asian activity at 1000 UT and a lesser amount of American activity at 0100 UT. There are obvious uncertainties in the application of these average results to our specific data; it appears reasonable, nevertheless, to associate the 0100 UT maximum in median amplitudes with thunderstorm activity in the Americas and the 1000 UT maximum with activity in S-E Asia.

Both maximums are greatly reduced by the SPE. For example, the median amplitudes during the hour 0100-0200 UT on 10 and 11 June are reduced by 46% and 58% compared with the corresponding average median amplitudes calculated for the same hour from the data in the 56-hour interval preceding the start of the SPE. There is also a reduction in the minimum median amplitudes. For example, if we make the same comparison as that just described for the two-hour interval 1600-1800 UT, when the median amplitudes normally pass through their lowest values, we find that the median amplitudes are reduced by 41% on 9 June and by 8% on 10 June.

The data for the categories of small, medium, and large sferics have variations that are very similar to the variation for all sferics.

Together, these variations suggest that the strongest SPE effects occur in the first 24 hours of the SPE and that the activity ascribed to thunderstorms in S-E Asia and the Americas is about equally affected during this interval. Since the area enclosed by the southern auroral zone lies between Byrd Station and S-E Asia (Figure 2), whereas very little of this zone lies between Byrd and the Americas, this result also suggests that the region of the ionosphere disturbed by the energetic proton precipitation expanded beyond the limits of the auroral zone during 9-10 June.

It is particularly interesting to see signs of recovery of the median amplitudes on 11 June and the occurrence of a comparatively large maximum at 0100 UT on 12 June. As pointed out during the description of the Byrd Station data, a large magnetic storm was in progress on 11 June, and it was on this day that the Byrd Station riometer recorded the most intense absorption of the entire SPE.

V.2 RATE OF OCCURRENCE OF SFERICS

Figure 7 shows the rate of occurrence of 75 Hz sferics in the one-minute synoptic intervals throughout the period 7-12 June 1968. The most commonly occurring sferics are those we have classified as being small: their rate of occurrence is always at least twice as large as the rates for the medium and large sferics, and during the peak of their well-defined diurnal variation of occurrence the small sferics occur at a rate that is roughly twice the rate for medium and large sferics combined. The diurnal variation corresponds closely with the variation of worldwide thunderstorm activity (Reference 42), and its peaks also correspond closely with the median amplitude minimums in Figure 6.

There are several SPE-related points of interest in the data shown in Figure 7. First, the rate of occurrence of all sferics increases following the start of the SPE and remains at a higher level for about 24 hours. Second, the rate of occurrence of all sferics is decreased during the magnetic storm phase of the SPE. Finally, examination of the variations for the different size categories shows that, unlike the amplitude data, the rates of occurrence of the large

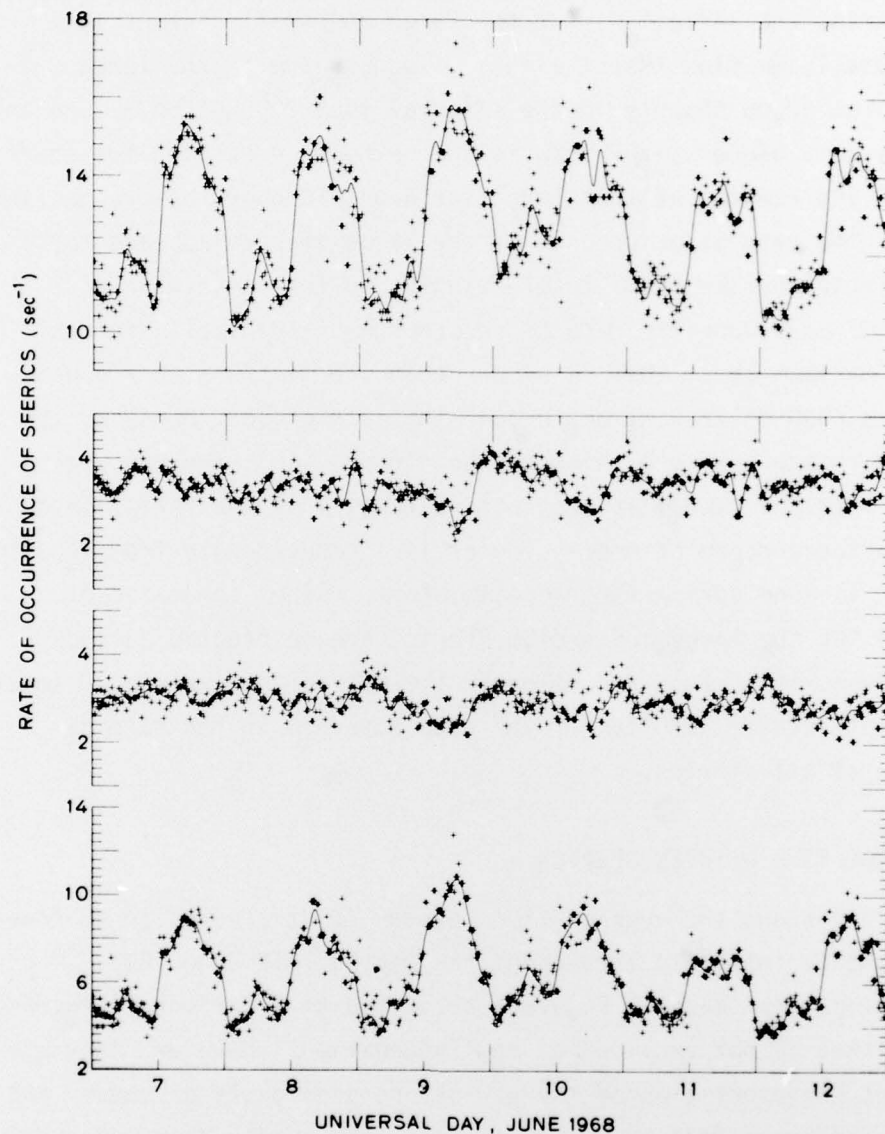


Figure 7. Variation of the rate of occurrence of 75 Hz sferics observed at Byrd Station, Antarctica, during the interval 7-12 June 1968. The top panel shows data for all sferics; the bottom panel shows data for small (bottom), medium (middle), and large (top) sferics.

and small sferics are affected differently by the SPE (the data for medium sferics show no obvious SPE effect).

Comparing the variations for the large and small sferics in greater detail, we find that the rate of occurrence of the large sferics first drops sharply in the interval 1400-2000 UT on 9 June and then rises to a higher level than in the 56 hours preceding the start of the SPE and remains at that level for about 12 hours before declining. Thereafter the rate of occurrence of the large sferics appears to be little affected by the SPE. Interestingly, in the same interval 1400-2000 UT on 9 June the rate of occurrence of the small sferics reaches a maximum level that is higher than the maximums on 7 and 8 June. From 0000 to 1200 UT on 10 June the rate of occurrence of the small sferics appears to be higher than normal, as is the case for the large sferics. The last distinctive feature of the variation in the rate of occurrence of small sferics is a reduced rate from 1200 to 2400 UT on 11 June during the magnetic storm. Since the rates of occurrence for the large and medium sferics are unaffected during the same interval, it is this reduction in the rate of occurrence of small sferics that accounts wholly for the drop observed in the rate of occurrence of all sferics.

V.3 AVERAGE TIME BETWEEN SFERICS

Figure 8 shows the average time between 75 Hz sferics in the one-minute synoptic intervals throughout the period 7-12 June 1968. These data are simply the data in Figure 7 presented in a different (inverse) form, and they do not provide any new information. However, they give a different representation of the variations previously discussed and emphasize different features. For example, the sudden change in the rate of occurrence of large sferics in the 24 hours following the start of the SPE is more obvious in Figure 8.

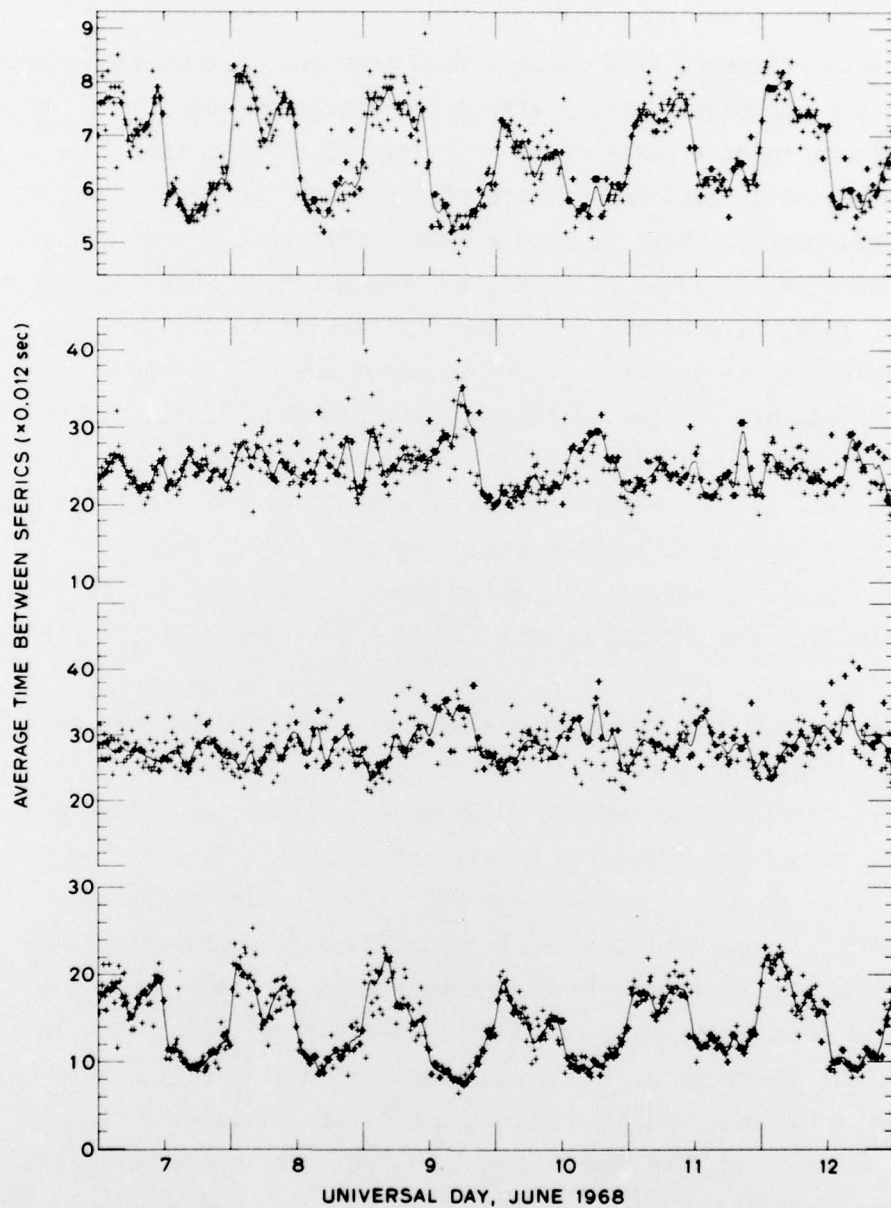


Figure 8. Variation of the average time between 75 Hz sferics observed at Byrd Station, Antarctica, during the interval 7-12 June 1968. The top panel shows data for all sferics; the bottom panel shows data for small (bottom), medium (middle), and large (top) sferics.

VI. DISCUSSION AND CONCLUSION

The data presented in Figures 6 to 8 show that a moderately large nighttime SPE can significantly affect the characteristics of 75 Hz sferics occurring at a polar location. The SPE effects include a reduction in median amplitude of the sferics, and changes in their rate of occurrence. There is some evidence that the largest SPE effects occur in the first 24 hours, before the start of the magnetic storm that forms part of the SPE. During these first 24 hours the spheric median amplitudes are reduced to about one-half of their earlier undisturbed values. Although this reduction is substantial, it is not sufficient to eliminate 75 Hz spheric occurrences at the polar location, i.e., there is no polar cap 'blackout' of the sferics. Also, the reduction appears to be no greater than the 4-8 db reductions in lower-ELF signal strength occasionally observed at lower latitudes in experiments with the Wisconsin Test Facility (References 10, 11, 13, 15, and 24).

Based on this study of a single SPE, we conclude that man-made lower-ELF signals propagating over paths passing through the polar regions are likely to be reduced in strength, although not severely (i.e., the reduction will be no greater than about 8 db), during the first 24 hours of a moderately large SPE. The changes occurring thereafter will depend on the characteristics of the magnetic storm phase of the SPE, which are likely to be highly variable, and on the position of the ELF receiver relative to the auroral zone. Our data suggests that the magnetic storm associated changes are likely to be no greater than those observed during the first 24 hours.

The start of an SPE is a particularly well-defined geophysical phenomenon: energetic ions, predominantly protons, suddenly begin arriving and creating ionization in the D-region of the ionosphere. Our observation of the simultaneous commencement of riometer absorption, signalling the start of an SPE, and of a Pc 3 pulsation event on 9 June 1968 is therefore of particular interest, since it may provide new information about the Pc 3 pulsation generation process. It appears

that the sudden creation of ionization in the ionospheric D-region either (1) provides the initial stimulation for a Pc 3 pulsation event, because of a new impulsive flow of current in the lower ionosphere, or (2) it provides more ideal conditions at the base of the ionosphere for the occurrence of a naturally stimulated Pc 3 event. We hope that further studies can be made of this relationship between SPE's and Pc 3 pulsations, including, as a first step, verification of the relationship by analysis of the pulsation activity that occurs during other SPE's.

It is desirable that the SPE measurements described in this communication be repeated using the controlled lower-ELF signals from the Wisconsin Test Facility and a unified satellite-ground station observational network similar to that described by Imhof et al. (Reference 24). Previous measurement programs in the northern hemisphere have usually involved few polar stations: greater use of polar stations would provide better information about the ionospheric region most strongly affected by SPE's and would facilitate interpretation of the SPE-related changes in the ELF signal measured at nonpolar locations. Finally, we note that a planned program of observations, including direction-finding, of naturally occurring ELF sferics at polar stations, and preferably at a minimum of two well-separated stations, could also provide much new information about SPE-effects on ELF signals in the polar regions. Natural sferics have two advantages over signals from man-made sources for this purpose. First, they are available at all times for measurement, and second, they reach a polar station from all directions. An optimum measurement program to determine the effects of an SPE on ELF signal propagation could well involve a combination of observations on the signals from the Wisconsin Test Facility at stations located in and around the northern polar region and observations of naturally occurring sferics either at the stations in the northern polar region or in the Antarctic.

VII. REFERENCES

1. Chapman, F. W., and R. C. V. Macario, "Propagation of audio-frequency radio waves to great distances," Nature, 177, 930, 1956.
2. Jean, A. G., A. C. Murphy, J. R. Wait, and D. F. Wasmundt, "Observed attenuation rate of ELF radio waves," J. Res. Natl. Bur. Stand., 65D, 475, 1961.
3. Bernstein, S. L., M. L. Burrows, J. E. Evans, A. S. Griffiths, D. A. McNeill, C. W. Niessen, I. Richer, D. P. White, and D. K. Willim, "Long-range communications at extremely low frequencies," Proc. IEEE, 62, 292, 1974.
4. Kruger, B., "Project Sanguine - FBM command and control communication," Naval Engrs. J., 84, 73, June 1972.
5. Wait, J. R., "Project Sanguine," Science, 178, 272, 1972.
6. Merrill, J., "Some early historical aspects of Project Sanguine," IEEE Trans. Commun., COM-22, 359, 1974.
7. Keiser, B. E., "Early development of the Project Sanguine radiating system," IEEE Trans. Commun., COM-22, 364, 1974.
8. Wait, J. R., "Propagation of ELF electromagnetic waves and Project Sanguine/Seafarer," IEEE J. Oceanic Engin., OE-2, 161, 1977.
9. White, D. P., and D. K. Willim, "Propagation measurements in the extremely low frequency (ELF) band," IEEE Trans. Commun., COM-22, 457, 1974.
10. Bannister, P. R., "Variations in extremely low frequency propagation parameters," J. Atmosph. Terr. Phys., 37, 1203, 1975.
11. Bannister, P. R., "Nighttime variations of extremely low frequency (ELF) signal strengths in Connecticut," IEEE Trans. Commun., COM-22, 474, 1974.
12. Bannister, P. R., and F. J. Williams, "Further examples of the nighttime variations of ELF signal strengths in Connecticut," J. Atmosph. Terr. Phys., 38, 313, 1976.
13. Davis, J. R., "The influence of certain ionospheric phenomena on extremely low frequency (ELF) propagation," IEEE Trans. Commun., COM-22, 484, 1974.

14. Davis, J. R., "ELF propagation irregularities on northern and mid-latitude paths," in ELF-VLF Radio Wave Propagation, edited by J. A. Holtet, 263-277, D. Reidel, Dordrecht, Holland, 1974.
15. Davis, J. R., "Localized nighttime D-region disturbances and ELF propagation," J. Atmosph. Terr. Phys., 38, 1309, 1976.
16. Larsen, T. R., "Preliminary discussion of ELF and VLF propagation data," in ELF-VLF Radio Wave Propagation, edited by J. A. Holtet, 285-289, D. Reidel, Dordrecht, Holland, 1974.
17. Bailey, D. K., "Polar-cap absorption," Planet. Space Sci., 12, 495, 1964.
18. Reid, G. C., "Current problems in polar-cap absorption," in Intercorrelated Satellite Observations Related to Solar Events, edited by V. Manno and D. E. Page, 319-334, D. Reidel, Dordrecht, Holland, 1970.
19. Reid, G. C., "Polar cap absorption - observations and theory," in Handbook of Astronomy, Astrophysics and Geophysics. Volume 1, edited by C. W. Gordon, V. Canuto, and W. I. Axford, 269-302, Gordon and Breach, New York, 1978.
20. Zmuda, A. J., and T. A. Potemra, "Bombardment of the polar-cap ionosphere by solar cosmic rays," Rev. Geophys. Space Sci., 10, 981, 1972.
21. Reagan, J. B., and T. M. Watt, "Simultaneous satellite and radar studies of the D region ionosphere during the intense solar particle events of August 1972," J. Geophys. Res., 81, 4579, 1976.
22. Crain, C. M., and H. G. Booker, "The effects of ions on low frequency and very low frequency propagation in an abnormally ionized atmosphere," J. Geophys. Res., 69, 4713, 1964.
23. Field, E. C., "Propagation of ELF waves under normal and naturally disturbed conditions," J. Geophys. Res., 74, 3639, 1969.
24. Imhof, W. L., J. B. Reagan, E. E. Gaines, T. R. Larsen, J. R. Davis, and W. Moler, "Coordinated measurements of ELF transmission anomalies and the precipitation of energetic particles into the ionosphere," Radio Sci., 13, 717, 1978.
25. Helliwell, R. A., J. P. Katsufakis, and M. L. Trimpi, "Whistler-induced amplitude perturbation in VLF propagation," J. Geophys. Res., 78, 4679, 1973.

26. Pappert, R. A., and W. F. Moler, "Propagation theory and calculations at lower extremely low frequencies (ELF)," IEEE Trans. Commun., COM-22, 438, 1974.
27. Smart, D. F., and M. A. Shea, "Solar proton event classification system," Solar Phys., 16, 484, 1971.
28. Hultqvist, B., "Polar cap absorption and ground level effects," in Solar Flares and Space Research, edited by C. de Jager and Z. Švestka, 215-257, North Holland, Amsterdam, 1969.
29. Švestka, Z., Solar Flares, 240, D. Reidel, Dordrecht, Holland, 1976.
30. Dodson-Prince, H. W., and A. Bruzek, "Flares and associated phenomena," in Illustrated Glossary for Solar and Solar-Terrestrial Physics, edited by A. Bruzek and C. J. Durrant, 81-96, D. Reidel, Dordrecht, Holland, 1977.
31. Švestka, Z., and P. Simon (editors), Catalog of Solar Particle Events 1955-1969, 95, D. Reidel, Dordrecht, Holland, 1975.
32. Solar-Geophysical Data, ESSA, U.S. Department of Commerce, 1968.
33. Masley, A. J., and P. R. Satterblom, "A discussion of solar cosmic ray activity near sunspot maximum," Acta Phys. Hung., 29, suppl. 2, 513, 1970.
34. Swanson, E. R., C. P. Kugel, and E. J. Hendricks, "Omega measurements: Pyramid Rock and Opana, Oahu, Hawaii," Rep. NELC/TD 392, Naval Electronics Laboratory Center, San Diego, Calif., 1975.
35. Morozumi, H. M., and R. A. Helliwell, "A correlation study of the diurnal variation of upper atmospheric phenomena in the southern auroral zone," Rep. SEL-66-124, Stanford Electron. Lab., Stanford Univ., Stanford, Calif., December 1966.
36. Reid, G. C., and H. H. Sauer, "Evidence for nonuniformity of solar-proton precipitation over the polar caps," J. Geophys. Res., 72, 4383, 1967.
37. Morozumi, H. M., "Diurnal variation of aurora zone geophysical disturbances," Rept. Ionosphere Space Res. Japan, 19, 286, 1965.
38. Chivers, H. J. A., "Substorm observations at L = 4," in Proceedings of IAGA Meeting on Unmanned Observatories in Antarctica, edited by T. Nagata, 76-87, Nat. Inst. of Polar Res., Tokyo, Japan, 1976.

39. Jacobs, J. A., Geomagnetic Micropulsations, 179 pp., Springer, New York, 1970.
40. Siren, J. C., "Fast hissers: A form of magnetospheric radio emissions," Rep. SEL-74-042, Stanford Electron. Lab., Stanford Univ., Stanford, Calif., August 1974.
41. Larsen, T. R., "ELF noise measurements," in ELF-VLF Radio Wave Propagation, edited by J. A. Holtet, 233-238, D. Reidel, Dordrecht, Holland, 1974.
42. U.S. Air Force/Geophysics Research Directorate, Handbook of Geophysics, Revised Edition, Macmillan, New York, 1960.

DISTRIBUTION LIST

DEPARTMENT OF DEFENSE

Assistant Secretary of Defense
Comm, Cmd, Cont. & Intell
ATTN: Dir. of Intelligence Systems, J. Babcock
ATTN: C3IST&CCS, M. Epstein

Assistant to the Secretary of Defense
Atomic Energy
ATTN: Executive Assistant

Command & Control Technical Center
ATTN: C-650, G. Jones
ATTN: C-312, R. Mason
3 cy ATTN: C-650, W. Heidig

Defense Advanced Rsch. Proj. Agency
ATTN: TIO

Defense Communications Agency
ATTN: Code 101B
ATTN: Code 480
ATTN: Code 810, J. Barna
ATTN: Code 205
ATTN: Code R1033, M. Raffensperger

Defense Communications Engineer Center
ATTN: Code R720, J. Worthington
ATTN: Code R410, J. McLean
ATTN: Code R123

Defense Documentation Center
12 cy ATTN: DD

Defense Intelligence Agency
ATTN: DB-4C, E. O'Farrell
ATTN: DC-7D, W. Wittig
ATTN: DT-1B
ATTN: DB, A. Wise
ATTN: DT-5
ATTN: HQ-TR, J. Stewart

Defense Nuclear Agency
ATTN: STVL
ATTN: DDST
3 cy ATTN: RAAE
4 cy ATTN: TITL

Field Command
Defense Nuclear Agency
ATTN: FCPR

Field Command
Defense Nuclear Agency
Livermore Division
ATTN: FCPRL

Interservice Nuclear Weapons School
ATTN: TTV

Joint Chiefs of Staff
ATTN: J-3, WWMCCS Evaluation Office
ATTN: J-37
ATTN: C3S

Joint Strat. Tgt. Planning Staff
ATTN: JLTW-2
ATTN: JPST, G. Goetz

DEPARTMENT OF DEFENSE (Continued)

National Security Agency
ATTN: R-52, J. Skillman
ATTN: W-32, O. Bartlett
ATTN: B-3, F. Leonard

Undersecretary of Defense for Rsch., & Engrg.
ATTN: Strategic & Space Systems (OS)

WWMCCS System Engineering Org.
ATTN: R. Crawford

DEPARTMENT OF THE ARMY

Assistant Chief of Staff for Automation & Comm.
Department of the Army
ATTN: DAAC-ZT, P. Kenny

Atmospheric Sciences Laboratory
U.S. Army Electronics R&D Command
ATTN: DELAS-EO, F. Niles

BMD Systems Command
Department of the Army
2 cy ATTN: BMDSC-HW

Deputy Chief of Staff for Ops. & Plans
Department of the Army
ATTN: DAMO-RQC

Electronics Tech. & Devices Lab
U.S. Army Electronics R&D Command
ATTN: DELET-ER, H. Bomke

Harry Diamond Laboratories
Department of the Army
ATTN: DELHD-N-P, F. Wimenitz
ATTN: DELHD-I-TL, M. Weiner
ATTN: DELHD-N-RB, R. Williams
ATTN: DELHD-N-P

U.S. Army Comm.-Elec. Engrg. Instal. Agency
ATTN: CCC-CED-CCO, W. Neuendorf
ATTN: CCC-EMEC-PED, G. Lane
ATTN: CCC-EMEO, W. Nair

U.S. Army Communications Command
ATTN: CC-OPS-WR, H. Wilson
ATTN: CC-OPS-W

U.S. Army Communications R&D Command
ATTN: DRDCO-COM-RY, W. Kesselman

U.S. Army Foreign Science & Tech. Ctr.
ATTN: DRXST-SD

U.S. Army Materiel Dev. & Readiness Cmd.
ATTN: DRCLDC, J. Bender

U.S. Army Nuclear & Chemical Agency
ATTN: Library

U.S. Army TRADOC Systems Analysis Activity
ATTN: ATAA-TDC
ATTN: ATAA-TCC, F. Payan, Jr.
ATTN: ATAA-PL

DEPARTMENT OF THE ARMY (Continued)

U.S. Army Satellite Comm. Agency
ATTN: Document Control

DEPARTMENT OF THE NAVY

Joint Cruise Missile Project Office
Department of the Navy
ATTN: JCM-G-70

Naval Air Development Center
ATTN: Code 6091, M. Setz

Naval Air Systems Command
ATTN: PMA, 271

Naval Electronic Systems Command
ATTN: Code 501A
ATTN: Code 3101, T. Hughes
ATTN: PME 117-20
ATTN: PME 106-4, S. Kearney
ATTN: PME 117-211, B. Kruger
ATTN: PME 106-13, T. Griffin
ATTN: PME-117-2013, G. Burnhart

Naval Intelligence Support Ctr.
ATTN: NISC-50

Naval Ocean Systems Center
ATTN: Code 5322, M. Paulson
ATTN: Code 532, J. Bickel
ATTN: Code 8151, C. Baggett
3 cy ATTN: Code 5324, W. Moler

Naval Research Laboratory
ATTN: Code 6701, J. Brown
ATTN: Code 7555
ATTN: Code 6700, T. Coffey
ATTN: Code 6707, J. Davis
ATTN: Code 7500, B. Wald
ATTN: Code 7580

Naval Space Surveillance System
ATTN: J. Burton

Naval Surface Weapons Center
ATTN: Code F31

Naval Surface Weapons Center
ATTN: Code F-14, R. Butler

Naval Telecommunications Command
ATTN: Code 341

Office of Naval Research
ATTN: Code 421
ATTN: Code 420

Office of the Chief of Naval Operations
ATTN: OP 604C
ATTN: OP 941D
ATTN: OP 981N

Strategic Systems Project Office
Department of the Navy
ATTN: NSP-2141
ATTN: NSP-43
ATTN: NSP-2722, F. Wimberly

DEPARTMENT OF THE AIR FORCE

Aerospace Defense Command
Department of the Air Force
ATTN: DC, T. Long
ATTN: XPDQ
ATTN: XP

Air Force Avionics Laboratory
ATTN: AAD, W. Hunt
ATTN: AAD, A. Johnson

Air Force Geophysics Laboratory
ATTN: OPR-1, J. Ulwick
ATTN: PHI, J. Buchau
ATTN: LKB, K. Champion
ATTN: OPR, A. Stair
ATTN: PHP, J. Aarons
ATTN: PHP, J. Mullen

Air Force Weapons Laboratory
Air Force Systems Command
ATTN: DYC
ATTN: SUL

Air Logistics Command
Department of the Air Force
ATTN: OO-ALC/MM, R. Blackburn

Assistant Chief of Staff
Intelligence
Department of the Air Force
ATTN: INED

Assistant Chief of Staff
Studies & Analyses
Department of the Air Force
ATTN: AF/SASC, G. Zank
ATTN: AF/SASC, W. Adams

Deputy Chief of Staff
Operations, Plans & Readiness
Department of the Air Force
ATTN: AFSOKCD
ATTN: AFXOXFD
ATTN: AFXOKS
ATTN: AFXOKT

Deputy Chief of Staff
Research, Development and Acq.
Department of the Air Force
ATTN: AFRDS
ATTN: AFRDSP
ATTN: AFRDSS
ATTN: AFRDQ

Electronic Systems Division
Department of the Air Force
ATTN: DCKC, J. Clark
ATTN: XRW, J. Deas
ATTN: YSM, J. Kobelski
ATTN: YSEA

Foreign Technology Division
Air Force Systems Command
ATTN: NIIS Library
ATTN: SDEC, A. Oakes
ATTN: TQTD, B. Ballard

DEPARTMENT OF THE AIR FORCE (Continued)

Rome Air Development Center
Air Force Systems Command
ATTN: OCS, V. Coyne
ATTN: TSLD

Rome Air Development Center
Air Force Systems Command
ATTN: EEP

Space & Missile Systems Organization
Air Force Systems Command
ATTN: MNNH
ATTN: MNNL, S. Kennedy

Space & Missile Systems Organization
Air Force Systems Command
ATTN: SKA, M. Clavin
ATTN: SKA, C. Rightmyer
ATTN: SZJ, L. Doan

Strategic Air Command
Department of the Air Force
ATTN: DCXT
ATTN: DCX
ATTN: DCXF
ATTN: OOKSN
ATTN: XPFS
ATTN: DCXT, T. Jorgensen
ATTN: NRT

OTHER GOVERNMENT AGENCIES

Central Intelligence Agency
ATTN: OSI/PSTD

Department of Commerce
National Bureau of Standards
ATTN: R. Moore

Department of Commerce
National Oceanic & Atmospheric Admin.
ATTN: Aeronomy Lab, G. Reid
ATTN: R. Grubb

Institute for Telecommunications Sciences
National Telecommunications & Info. Admin.
ATTN: A. Jean
ATTN: W. Utlaut
ATTN: L. Berry
ATTN: D. Crombie

U.S. Coast Guard
Department of Transportation
ATTN: G-DOE-3/TP54, B. Romine

DEPARTMENT OF ENERGY CONTRACTORS

Lawrence Livermore Laboratory
ATTN: Technical Information Dept. Library

Los Alamos Scientific Laboratory
ATTN: D. Westervelt
ATTN: P. Keaton
ATTN: T. Taschek

Sandia Laboratories
Livermore Laboratory
ATTN: T. Cook
ATTN: B. Murphey

DEPARTMENT OF ENERGY CONTRACTORS (Continued)

Sandia Laboratories
ATTN: Org. 1250, W. Brown
ATTN: D. Dahlgren
ATTN: 3141
ATTN: Space Project Div.
ATTN: D. Thornbrough

DEPARTMENT OF DEFENSE CONTRACTORS

Aerospace Corp.
ATTN: S. Bower
ATTN: D. Olsen
ATTN: N. Stockwell
ATTN: F. Morse
ATTN: V. Josephson
ATTN: I. Garfunkel
ATTN: R. Slaughter
ATTN: T. Salmi

University of Alaska
Geophysical Institute
ATTN: T. Davis
ATTN: N. Brown
ATTN: Technical Library

Analytical Systems Engineering Corp.
ATTN: Radio Sciences

Analytical Systems Engineering Corp.
ATTN: Security

Barry Research Communications
ATTN: J. McLaughlin

BDM Corp.
ATTN: T. Neighbors
ATTN: L. Jacobs

Berkeley Research Associates, Inc.
ATTN: J. Workman

Boeing Co.
ATTN: D. Murray
ATTN: G. Hall
ATTN: S. Tashird
ATTN: J. Kenney

University of California at San Diego
ATTN: H. Booker

Charles Stark Draper Lab., Inc.
ATTN: D. Cox
ATTN: J. Gilmore

Computer Sciences Corp.
ATTN: H. Blank

Comsat Labs
ATTN: G. Hyde
ATTN: R. Taur

Cornell University
ATTN: D. Farley, Jr.

EG&G, Inc.
ATTN: Document Control for J. Colvin
ATTN: Document Control for D. Wright

DEPARTMENT OF DEFENSE CONTRACTORS (Continued)

Electrospace Systems, Inc.
ATTN: H. Logston

ESL, Inc.
ATTN: J. Marshall
ATTN: C. Prettie
ATTN: J. Roberts

Ford Aerospace & Communications Corp.
ATTN: J. Mattingley

General Electric Co.
ATTN: M. Bortner

General Electric Co.
ATTN: A. Steinmayer
ATTN: C. Zierdt
ATTN: S. Lipson

General Electric Co.
ATTN: F. Reibert

General Electric Company—TEMPO
ATTN: T. Stevens
ATTN: M. Stanton
ATTN: DASIAC
ATTN: W. Knapp
ATTN: D. Chandler

General Electric Tech. Services Co., Inc.
ATTN: G. Millman

General Research Corp.
ATTN: J. Garbarino
ATTN: J. Ise, Jr.

GTE Sylvania, Inc.
ATTN: M. Cross

HSS, Inc.
ATTN: D. Hansen

IBM Corp.
ATTN: F. Ricci

University of Illinois
ATTN: K. Yeh

Institute for Defense Analyses
ATTN: J. Bengston
ATTN: E. Bauer
ATTN: J. Aein
ATTN: H. Wolfhard

International Tel. & Telegraph Corp.
ATTN: G. Wetmore
ATTN: Technical Library

JAYCOR
ATTN: S. Goldman

JAYCOR
ATTN: D. Carlos

Kaman Sciences Corp.
ATTN: T. Meagher

Linkabit Corp.
ATTN: I. Jacobs

DEPARTMENT OF DEFENSE CONTRACTORS (Continued)

Johns Hopkins University
ATTN: Document Librarian
ATTN: T. Potemra
ATTN: B. Wise
ATTN: T. Evans
ATTN: J. Newland
ATTN: P. Komiske

Litton Systems, Inc.
ATTN: R. Grasty

Lockheed Missiles & Space Co., Inc.
ATTN: D. Churchill
ATTN: Dept. 60-12

Lockheed Missiles and Space Co., Inc.
ATTN: R. Johnson
ATTN: W. Imhof
ATTN: M. Walt

M.I.T. Lincoln Lab.
ATTN: D. Towle
ATTN: L. Loughlin

McDonnell Douglas Corp.
ATTN: G. Mroz
ATTN: W. Olson
ATTN: N. Harris
ATTN: J. Moule

Mission Research Corp.
ATTN: R. Bogusch
ATTN: S. Gutsche
ATTN: D. Sowle
ATTN: R. Hendrick
ATTN: M. Scheibe
ATTN: F. Fajen

Mitre Corp.
ATTN: G. Harding
ATTN: C. Callahan
ATTN: A. Kymmel

Mitre Corp.
ATTN: M. Horrocks
ATTN: W. Foster
ATTN: W. Hall

Pacific-Sierra Research Corp.
ATTN: E. Field, Jr.

Pennsylvania State University
ATTN: Ionospheric Research Lab.

Photometrics, Inc.
ATTN: I. Kofsky

Physical Dynamics, Inc.
ATTN: E. Fremouw

R&D Associates
ATTN: L. Delaney

Radio Science Laboratory
Stanford University
ATTN: A. Frazer-Smith
ATTN: R. Helliwell

DEPARTMENT OF DEFENSE CONTRACTORS (Continued)

R&D Associates

ATTN: R. Lelevier
ATTN: M. Gantsweg
ATTN: H. Ory
ATTN: R. Turco
ATTN: C. Greifinger
ATTN: W. Wright, Jr.
ATTN: B. Gabbard
ATTN: W. Karzas
ATTN: C. MacDonald
ATTN: F. Gilmore

Rand Corp.

ATTN: C. Crain
ATTN: E. Bedrozian

Riverside Research Institute

ATTN: V. Trapani

Rockwell International Corp.

ATTN: J. Kristof

Santa Fe Corp.

ATTN: E. Ortlieb

Science Applications, Inc.

ATTN: C. Smith
ATTN: D. Hamlin
ATTN: D. Sachs
ATTN: J. McDougall
ATTN: E. Straker
ATTN: L. Linson

Science Applications, Inc.

ATTN: D. Divis

DEPARTMENT OF DEFENSE CONTRACTORS (Continued)

Science Applications, Inc.

ATTN: SZ

SRI International

ATTN: A. Burns
ATTN: G. Price
ATTN: R. Leadabrand
ATTN: R. Livingston
ATTN: M. Baron
ATTN: G. Carpenter
ATTN: C. Rino
ATTN: W. Jaye
ATTN: W. Chesnut
ATTN: D. Neilson
ATTN: G. Smith

Teledyne Brown Engineering

ATTN: R. Deliberis

Tri-Com, Inc.

ATTN: D. Murray

TRW Defense & Space Sys. Group

ATTN: S. Altschuler
ATTN: R. Plebuch
ATTN: D. Dee

Utah State University

ATTN: L. Jensen
ATTN: K. Baker

Visidyne, Inc.

ATTN: J. Carpenter